The closure of Pak1-dependent macropinosomes requires the phosphorylation of CtBP1/BARS

Prisca Liberali[1], Elina Kakkonen[2], Gabriele Turacchio[3], Carmen Valente[1], Alexander Spaar[3], Giuseppe Perinetti[1], Rainer A Böckmann[4], Daniela Corda[1], Antonino Colanzi[1,*], Varpu Marjomaki[2] and Alberto Luini[3,*]

[1]Laboratory of Cell Regulation, Department of Cell Biology and Oncology, Consorzio Mario Negri Sud, Santa Maria Imbaro (Chieti), Italy, [2]Department of Biological and Environmental Science, Nanoscience Centre, University of Jyvaskyla, Jyvaskyla, Finland, [3]Laboratory of Membrane Traffic, Department of Cell Biology and Oncology, Consorzio Mario Negri Sud, Santa Maria Imbaro (Chieti), Italy and [4]Theoretical and Computational Membrane Biology, Centre for Bioinformatics, Saarland University, Saarbruecken, Germany

Membrane fission is an essential process in membrane trafficking and other cellular functions. While many fissioning and trafficking steps are mediated by the large GTPase dynamin, some fission events are dynamin independent and involve C-terminal-binding protein-1/brefeldinA-ADP ribosylated substrate (CtBP1/BARS). To gain an insight into the molecular mechanisms of CtBP1/BARS in fission, we have studied the role of this protein in macropinocytosis, a dynamin-independent endocytic pathway that can be synchronously activated by growth factors. Here, we show that upon activation of the epidermal growth factor receptor, CtBP1/BARS is (a) translocated to the macropinocytic cup and its surrounding membrane, (b) required for the fission of the macropinocytic cup and (c) phosphorylated on a specific serine that is a substrate for p21-activated kinase, with this phosphorylation being essential for the fission of the macropinocytic cup. Importantly, we also show that CtBP1/BARS is required for macropinocytic internalization and infection of echovirus 1. These results provide an insight into the molecular mechanisms of CtBP1/BARS activation in membrane fissioning, and extend the relevance of CtBP1/BARS-induced fission to human viral infection.

*Corresponding authors. A Colanzi, Laboratory of Cell Regulation, Department of Cell Biology and Oncology, Consorzio Mario Negri Sud, 66030 Santa Maria Imbaro (Chieti), Italy. Tel.: +39 0872 570310; Fax: +39 0872 570412; E-mail: colanzi@negrisud.it or A Luini, Laboratory of Membrane Traffic, Department of Cell Biology and Oncology, Consorzio Mario Negri Sud, 66030 Santa Maria Imbaro (Chieti), Italy. Tel.: +39 0872 570355; Fax: +39 0872 570412; E-mail: luini@negrisud.it

Introduction

Membrane fission is an essential step in different cellular processes, including the formation of membrane traffic carriers and the partitioning of the Golgi complex during mitosis (Corda *et al*, 2006; McNiven and Thompson, 2006; Colanzi *et al*, 2007). While numerous fissioning and trafficking events involve the well-characterized large GTPase dynamin (Schmid *et al*, 1998; Conner and Schmid, 2003; Pelkmans and Helenius, 2003; Praefcke and McMahon, 2004; Newton *et al*, 2006; Ferguson *et al*, 2007), others have been shown to be dynamin independent (Sabharanjak *et al*, 2002; Glebov *et al*, 2006) and to require, at least in some cases, the C-terminal-binding protein-1/brefeldin A-ADP ribosylated substrate (CtBP1/BARS; Hidalgo Carcedo *et al*, 2004; Bonazzi *et al*, 2005; Yang *et al*, 2005; Corda *et al*, 2006).

CtBP1/BARS belongs to a dual-function protein family that is known to be involved in both membrane fission and gene transcription (Chinnadurai, 2003; Corda *et al*, 2006). As a nuclear transcription factor, CtBP1/BARS regulates numerous cellular functions, including epithelial differentiation, tumorigenesis and apoptosis (Chinnadurai, 2002; Grooteclaes *et al*, 2003). In the cytoplasm, CtBP1/BARS controls the fission machinery that is involved in the formation of post-Golgi carriers, endocytic fluid-phase carriers (Bonazzi *et al*, 2005) and COP1-coated vesicles (Yang *et al*, 2005); CtBP1/BARS is also involved in mitotic Golgi partitioning (Hidalgo Carcedo *et al*, 2004; Colanzi *et al*, 2007). Whether and how the nuclear and cytoplasmic functions of CtBP1/BARS are related remains so far unclear. The precise mechanism of action of CtBP1/BARS, and whether CtBP1/BARS has a direct mechanistic or regulatory role in membrane fission, also remains unclear. Thus, the phrase CtBP1/BARS-dependent fission will be used in this study to refer to the whole fissioning process, including its regulatory stages.

To gain an insight into the molecular mechanisms of CtBP1/BARS in fission, we have studied macropinocytosis, a dynamin-independent (and hence possibly CtBP1/BARS dependent) endocytic pathway (Meier *et al*, 2002; Pelkmans and Helenius, 2003; Kirkham and Parton, 2005). While macropinocytosis is constitutive in specialized antigen-presenting cells (Steinman and Swanson, 1995), it can also be rapidly and synchronously induced by growth factors in other cell types (Haigler *et al*, 1979; Mellstrom *et al*, 1988; West *et al*, 1989). This is advantageous for mechanistic studies, in that it can help to reveal fission-related CtBP1/BARS modifications and interactions that occur during stimulation.

Macropinocytosis is an essential aspect of normal cell function that contributes to a number of cellular processes, such as antigen sampling (Steinman and Swanson, 1995) and cell motility (Ahram *et al*, 2000). It results in the formation of large endocytic vesicles that originate from actin ruffles at the plasma membrane. This ruffling is followed by the invagination of the plasma membrane and the formation of a macropinocytic cup, which is then closed via the fissioning of its junction with the plasma membrane (its 'neck') (Swanson and Watts, 1995).

Here, we show that CtBP1/BARS has an essential role in the fission of the macropinosome neck during epidermal growth factor (EGF)-mediated macropinocytosis, and we analyse the mechanisms leading to CtBP1/BARS activation in this context. We thus show that, upon EGF receptor engagement, CtBP1/BARS is translocated to the macropinocytic cup and its surrounding membrane. In addition, during macropinocytosis, CtBP1/BARS is phosphorylated on a specific serine that is known to be a substrate of p21-activated kinase (Pak1), and this phosphorylation is essential for the fission of the macropinocytic cup. Importantly, we also show that CtBP1/BARS is required for the macropinocytic internalization and infection of echovirus 1 (EV1). Our study thus opens the way for further investigations into the molecular mechanisms of action of CtBP1/BARS in membrane fission and demonstrates the relevance of this process in human disease.

Results

CtBP1/BARS is required for EGF-stimulated macropinocytosis

To determine the role of CtBP1/BARS in macropinocytosis, we used an established *in-vivo* assay for EGF-stimulated macropinocytosis in human A431 epidermoid carcinoma cells (Hewlett *et al*, 1994; Hamasaki *et al*, 2004). The cells were incubated in serum-free buffer and then stimulated with EGF in the presence of TRITC-labelled dextran, to monitor macropinosome formation. In the absence of EGF, dextran was internalized into a few endosomes of variable sizes. The addition of EGF induced actin ruffling (Supplementary Figure 1A) and a strong stimulation of dextran uptake (Figure 1A), which increased with time and reached a plateau 8–10 min after EGF addition (Figure 1B). To establish whether this uptake was due to bona-fide macropinocytosis, we investigated the effects of the following macropinocytosis inhibitors: amiloride, a Na^+/H^+ exchange inhibitor (West *et al*, 1989); cytochalasin D, an actin depolymerizing agent (Amyere *et al*, 2002); wortmannin, a phosphoinositide 3-kinase (PI3K) inhibitor (Amyere *et al*, 2002); Go6976 and Ro31-8220, two protein kinase C (PKC) inhibitors (Swanson and Watts, 1995); BAPTA-AM, a cell-permeant calcium chelator (Falcone *et al*, 2006); and U73122, a phospholipase C (PLC) inhibitor (Amyere *et al*, 2002). In cells separately pretreated with each of these agents, dextran uptake was strongly inhibited (Supplementary Figure 1B). This inhibitory pattern is considered diagnostic of macropinocytosis (Schnatwinkel *et al*, 2004).

We then examined whether CtBP1/BARS is involved in macropinocytosis by using multiple approaches to inhibit CtBP1/BARS function. First, we targeted CtBP1/BARS by RNA interference in A431 cells. Notably, CtBP1/BARS exists as two splice variants that differ only in the absence of the first 11 amino acids from the N-terminus of the long isoform, CtBP1-L/BARS, which results in the short isoform, CtBP1-S/BARS. Of these, CtBP1-S/BARS has so far been characterized in membrane fission assays, whereas CtBP1-L/BARS has been characterized as a transcription factor (Chinnadurai, 2003; Corda *et al*, 2006), although their functions are in fact very likely to overlap (Corda *et al*, 2006). Our small-interfering RNAs (siRNAs) were designed to target both forms. They strongly reduced the overall CtBP1/BARS levels

(Supplementary Figure 1C) and markedly decreased macropinocytosis (Figure 1C and D) without affecting cell viability. To ascertain the specificity of these siRNAs, we sought to rescue macropinocytosis by first injecting each of the recombinant CtBP1/BARS–GST forms into CtBP1/BARS-depleted cells 1 h before the macropinocytosis assay. Both CtBP1-S/BARS–GST (Figure 1C and D) and CtBP1-L/BARS–GST (data not shown) substantially restored EGF-stimulated macropinocytosis. Moreover, the two isoforms were equally active in other CtBP1/BARS-dependent fissioning events (Corda *et al*, 2006) (data not shown). From hereafter, therefore, we will refer to both proteins as CtBP1/BARS, unless specified otherwise.

Second, we inhibited CtBP1/BARS acutely, by injecting cells with two recombinant deletion mutants of CtBP1/BARS that have previously been shown to act as dominant-negative (DN) mutants, that is, the CtBP1/BARS nucleotide-binding domain (NBD, which blocks cargo export from the Golgi complex; Bonazzi *et al*, 2005) and the substrate-binding domain (SBD, which blocks mitotic Golgi partitioning, but has no effects on Golgi trafficking; Hidalgo Carcedo *et al*, 2004). Both of these DN mutants strongly inhibited the formation of macropinosomes (Figure 1E and F), indicating that CtBP1/BARS is required for EGF-stimulated macropinocytosis. Also of note here is that, first, the effects of the CtBP1/BARS DN SBD mutant on macropinocytosis may not follow changes in trafficking out of the Golgi complex, as SBD has no inhibitory effect on Golgi export (Bonazzi *et al*, 2005), and second, the inhibitory action of the DN mutants in microinjection experiments is too rapid to be mediated by the transcriptional effects of these CtBP1/BARS mutants (less than 1 h). In addition, we injected cells with a previously characterized anti-CtBP1/BARS blocking antibody that recognizes both CtBP1/BARS isoforms (Hidalgo Carcedo *et al*, 2004; Bonazzi *et al*, 2005). Again, this resulted in strong inhibition of macropinocytosis, as compared to IgG-injected cells (Figure 1G and H).

In parallel, we carried out a series of control experiments. First, as macropinocytosis originates from ruffling, we examined whether the inhibition/depletion of CtBP1/BARS by each of the above treatments affects the actin cytoskeleton: none of them showed detectable effects on actin, either in the absence or presence of EGF (Supplementary Figure 1D). Second, we examined the effects of acutely enhancing the cellular CtBP1/BARS levels by microinjecting native CtBP1/BARS into control cells: this did not increase or otherwise alter the macropinocytic response upon EGF stimulation, indicating that endogenous CtBP1/BARS is sufficient (i.e., non-rate-limiting) for a full macropinocytic response (Figure 1C and D). Finally, we observed that long exposures (24 h) of the cells to enhanced levels of CtBP1/BARS achieved by microinjection of recombinant CtBP1-S/BARS–GST or overexpression of CtBP1-S/BARS–YFP (see Supplementary Figure 1E) partially reduced the macropinocytic response to EGF (Supplementary Figure 1E), similar to the inhibitory effect seen previously for secretory trafficking (Bonazzi *et al*, 2005).

Upon EGF stimulation, CtBP1/BARS is recruited to actin-rich membrane ruffles and to the macropinocytic cup

To analyse the role of CtBP1/BARS in macropinocytosis, we performed video microscopy for both actin and CtBP1/BARS.
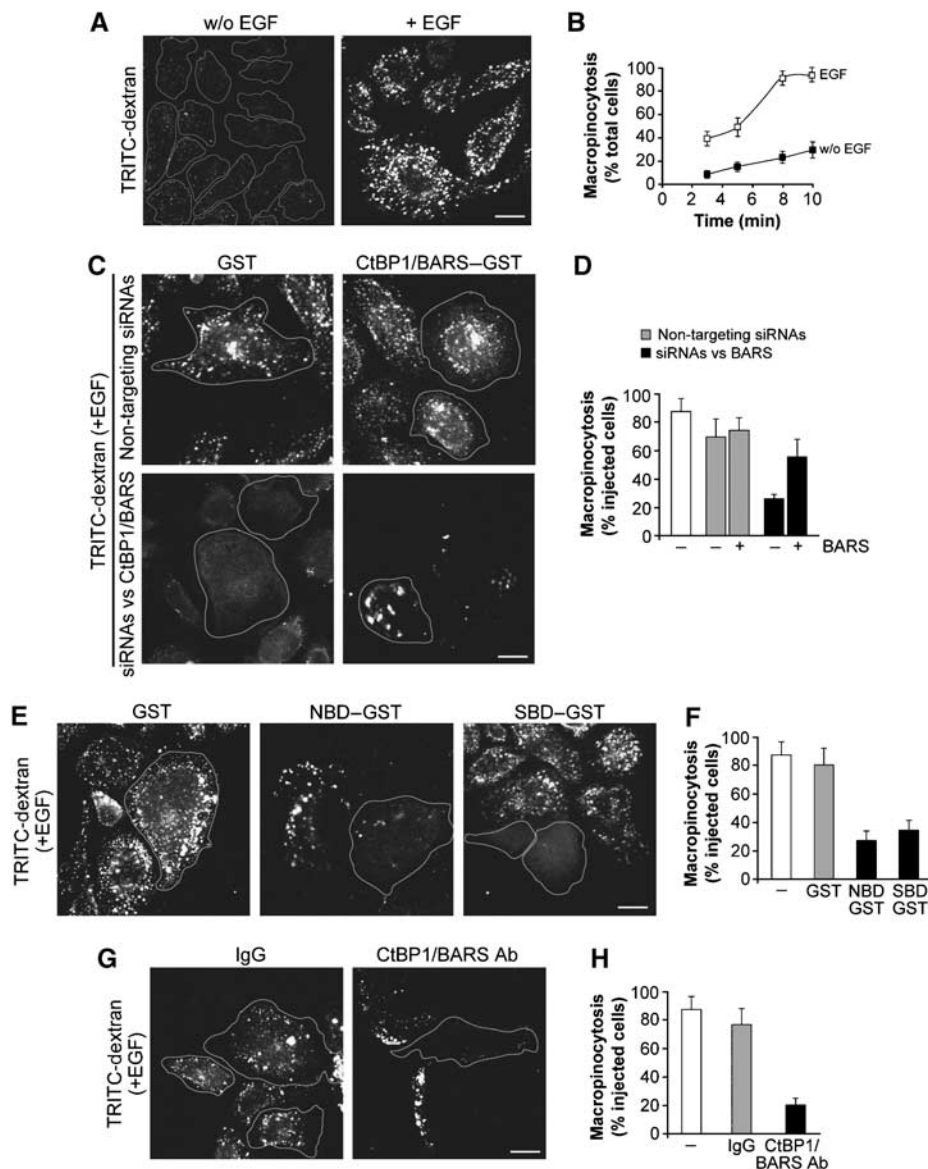
Figure 1 CtBP1/BARS is required for EGF-stimulated macropinocytosis in A431 cells. (**A**) Cells were incubated for 1 h in serum-free Ringer's buffer and for 8 min in Ringer's buffer containing TRITC-conjugated dextran in the absence (w/o) or presence (+) of 50 ng/ml EGF. After fixing, the cells were examined under confocal microscopy for macropinocytosis. (**B**) Quantification of macropinocytosing cells treated as in (A), as indicated (see Materials and methods). (**C**) Cells were transfected for 72 h with non-targeting siRNAs or siRNAs targeted to CtBP1/BARS, and injected with GST or wild-type CtBP1-S/BARS–GST, as indicated. One hour later, they were incubated for 1 h in serum-free Ringer's buffer and then for 8 min in Ringer's buffer containing 50 ng/ml EGF and TRITC-conjugated dextran. Injected cells are outlined. (**D**) Quantification of macropinocytosing cells treated as in (C), as indicated (see Materials and methods). (**E**) Cells were microinjected with GST, NBD or SBD, as indicated, and processed as in (C). (**F**) Quantification of macropinocytosing cells treated as in (E), as indicated (see Materials and methods). (**G**) Cells were either untreated (not shown), or injected with IgG or the blocking p50-2 anti-CtBP1/BARS antibody (CtBP1/BARS Ab), as indicated, and 1 h later they were processed as in (C). (**H**) Quantification of macropinocytosing cells treated as in (G), as indicated (see Materials and methods). More than 100 cells were analysed under each experimental condition, and the data are means ± s.d. from three independent experiments. Scale bars: 10 μm.

The actin dynamics in living cells were monitored using the actin-binding domain of filamin fused to GFP (ABD-filamin–GFP) (Figure 2A). This marker confirmed the effects of EGF on the actin cytoskeleton, and also allowed visualization of forming macropinocytic cups: segments of the membrane in the ruffling area retracted (invaginated) towards the cell interior to form cup-shaped structures (0.5–2.0 μm in diameter) that persisted for variable times (60–90 s) (Figure 2A, arrowheads). These appeared to narrow around their orifice and then to close (Figure 2A, arrow). Simultaneously, the internalized macropinosomes lost their fluorescent actin marker (Figure 2A, lower panel). This is similar to previous descriptions, and it confirms that actin localization at the macropinocytic cup is transient, lasting only until the closure of the macropinosome (Lee and Knecht, 2002; Schnatwinkel et al, 2004).

We then examined the localization of CtBP1/BARS during EGF stimulation, by immunofluorescence. In quiescent cells, CtBP1/BARS was both nuclear and cytoplasmic (Figure 2B, control). Upon addition of EGF, CtBP1/BARS moved to the forming membrane ruffles (Figure 2B), which were rich in

F-actin, and also to round structures within the ruffling areas that were reminiscent of macropinocytic cups (Figure 2B, arrows). Notably, the overlap of the actin ruffles with CtBP1/BARS at the plasma membrane was nearly perfect at all times after EGF stimulation, indicating that CtBP1/BARS is recruited on these ruffles as soon as they form. To monitor the living dynamics of CtBP1-S/BARS, we used a fluorescent-tagged construct (CtBP1-S/BARS–YFP) and examined the cells under the confocal microscope 6 h after transfection. CtBP1-S/BARS–YFP showed a localization that was similar to that of the endogenous protein in both quiescent and EGF-stimulated cells (not shown). Upon EGF stimulation, CtBP1-S/BARS–YFP translocated onto the membrane ruffles and the cup-shaped structures that developed from the ruffles (see Supplementary Movies 1 and 2). These structures, and the associated CtBP1-S/BARS–YFP, persisted for less than 90 s before closing (Figure 2C, white arrows, 90–200 s), with this coinciding with the detachment of CtBP1-S/BARS–YFP from the macropinocytic cup. The large round macropinosomes that formed from these cups then moved rapidly into the cell (confirming the macropinocytic nature of the cups) (Figure 2C, arrowheads, 200–300 s). A detailed inspection of this closure event revealed that the detachment of CtBP1/BARS–YFP initiated at the base of the cup (Figure 2C, black arrows, 120–200 s) and coincided with its transient enrichment at the neck, where the fissioning of the macropinosome occurs (Figure 2C, white arrows, 180–200 s).

To confirm this enrichment on the plasma-membrane ruffles and macropinocytic cups, the localization of CtBP1-S/BARS–YFP in EGF-stimulated cells was analysed by immuno-electron microscopy (EM). As shown in Figure 2D, CtBP1/BARS–YFP was strongly enriched in ruffling areas of the plasma membrane, as compared to other areas (Figure 2D, arrows).

CtBP1/BARS is specifically required for the fission of the macropinocytic cup

Having established an essential role for CtBP1/BARS in macropinocytosis, we next sought to determine its site of action. In principle, CtBP1/BARS could act at the following steps: (i) formation of actin-dependent membrane ruffles; (ii) invagination of the macropinocytic cup; and/or (iii) fission of the macropinosome neck. The first possibility can be excluded, as under all conditions investigated the inhibition or ablation of CtBP1/BARS had no apparent effects on actin ruffling (Supplementary Figure 1D). We thus sought to distinguish whether CtBP1/BARS acts by controlling the formation or the fission of the macropinocytic cup, by using multiple approaches.

In the first approach, we modified the macropinocytosis assay as follows: we fixed the cells without prior washing (instead of washing them extensively, as for the previous experiments in Figure 1C–F), so as not to remove the dextran present in the invaginated cups; moreover, we used fluorescein-conjugated 'fixable' lysine-containing dextran (FITC-dextran). While under the 'extensive washing' conditions used in previous experiments, the number of macropinosomes was strongly reduced in CtBP1/BARS-inhibited cells (e.g., by injection of the DN NBD mutant) (Figure 3B), under these 'no wash' conditions, the CtBP1/BARS-inhibited cells showed a number of dextran-positive round macropinosome-like structures that were comparable to those seen in control

cells (Figure 3A, upper panels, and Figure 3B). This suggests that in these inhibited cells, macropinocytic cups can form but cannot develop into complete macropinosomes.

To test this conclusion more directly, we exposed the fixed cells to a pH 5.0 medium, exploiting the pH sensitivity of the fluorescence of FITC-dextran, which is quenched below pH 5.5. The rationale here is that under these conditions, the macropinocytic cups that were still connected with the plasma membrane should lose their fluorescence, whereas the sealed macropinosomes should not. Strikingly, the vast majority of the dextran-positive macropinosome-like structures in these CtBP1/BARS-inhibited cells indeed showed a consistent bleaching of fluorescence after acidification, indicating that these structures were still connected with the extracellular space (Figure 3A and C). In contrast, in control (GST-injected) cells, a much smaller fraction of the dextran-positive structures showed this loss of fluorescence (Figure 3A and C). Similar results were obtained using TRITC-dextran conjugated with biotin as the fluid-phase marker and Alexa633-conjugated streptavidin as a probe to test the accessibility of extracellular molecules to the macropinosomal lumen after fixation. Under these conditions, the macropinosomes that were formed in the presence of the CtBP1/BARS DN mutant NBD again remained accessible to the external medium (Figure 3D and E). Thus, these data indicate that in cells where CtBP1/BARS function is impaired, the macropinocytic cup is formed normally whereas fission is inhibited.

As a third approach, A431 cells were transfected with the CtBP1/BARS DN mutant NBD–YFP, to follow its living dynamics after EGF stimulation. The rationale here was that if this inhibitory construct localizes to the macropinocytic cups like CtBP1/BARS, it should allow visualization of cups that are unable to close. Indeed, upon EGF stimulation, NBD–YFP was seen on plasma membrane ruffles and cup-like structures (see Supplementary Movies 3 and 4). However, these cups did not develop into macropinosomes and NBD–YFP remained on their surface often for long times (up to 200 s), until the cup 'aborted' into a normal plasma membrane ruffle (Figure 3F, 90–320 s, arrow). These results confirm that CtBP1/BARS is required for macropinosome closure.

CtBP1/BARS is required for EV1 internalization and infection

Next, we examined the role of CtBP1/BARS in the 'macropinocytosis-like' internalization of EV1. This choice was both because of the intrinsic interest of the viral entry process and because the macropinocytic structures involved in EV1 internalization can be conveniently characterized by EM (see below). EV1 is a small, non-enveloped, RNA-containing picornavirus that can cause meningitis, encephalitis and mild respiratory and enteric infections in humans (Grist *et al*, 1978). The internalization of EV1 has been recently characterized and shown to be mediated by the binding of the virus to $\alpha_2\beta_1$ integrins (Upla *et al*, 2004), which then cluster and trigger viral entry. As this internalization process involves the same players as those that mediate EGF-dependent macropinocytosis (e.g., Pak1, Rac1, PLC, PI3K, PKC, the actin cytoskeleton) (Karjalainen *et al*, 2008), it is thought to be macropinocytic in nature (also, see below).

We first examined whether EV1 internalization is CtBP1/BARS dependent by injecting SAOS cells (that stably express

$\alpha_2\beta_1$ integrins) with the CtBP1/BARS DN SBD mutant and then exposing the cells to EV1. Quantitative immuno-fluorescence analysis (see Materials and methods) of the internalized versus the plasma-membrane-bound viral particles indicated that SBD resulted in a strong inhibition (greater than 70%) of EV1 internalization (Figure 4C and D). We also tested whether infection by EV1 (as assessed

with a primary antibody against EV1) requires CtBP1/BARS, by injecting SAOS cells with the CtBP1/BARS DN NBD and SBD mutants. Indeed, these DN-microinjected cells showed clearly reduced levels of EV1 infection (Figure 4A). As a control experiment, we also examined the effects of CtBP1/BARS inhibition on infection by a virus internalized through a macropinocytosis-independent
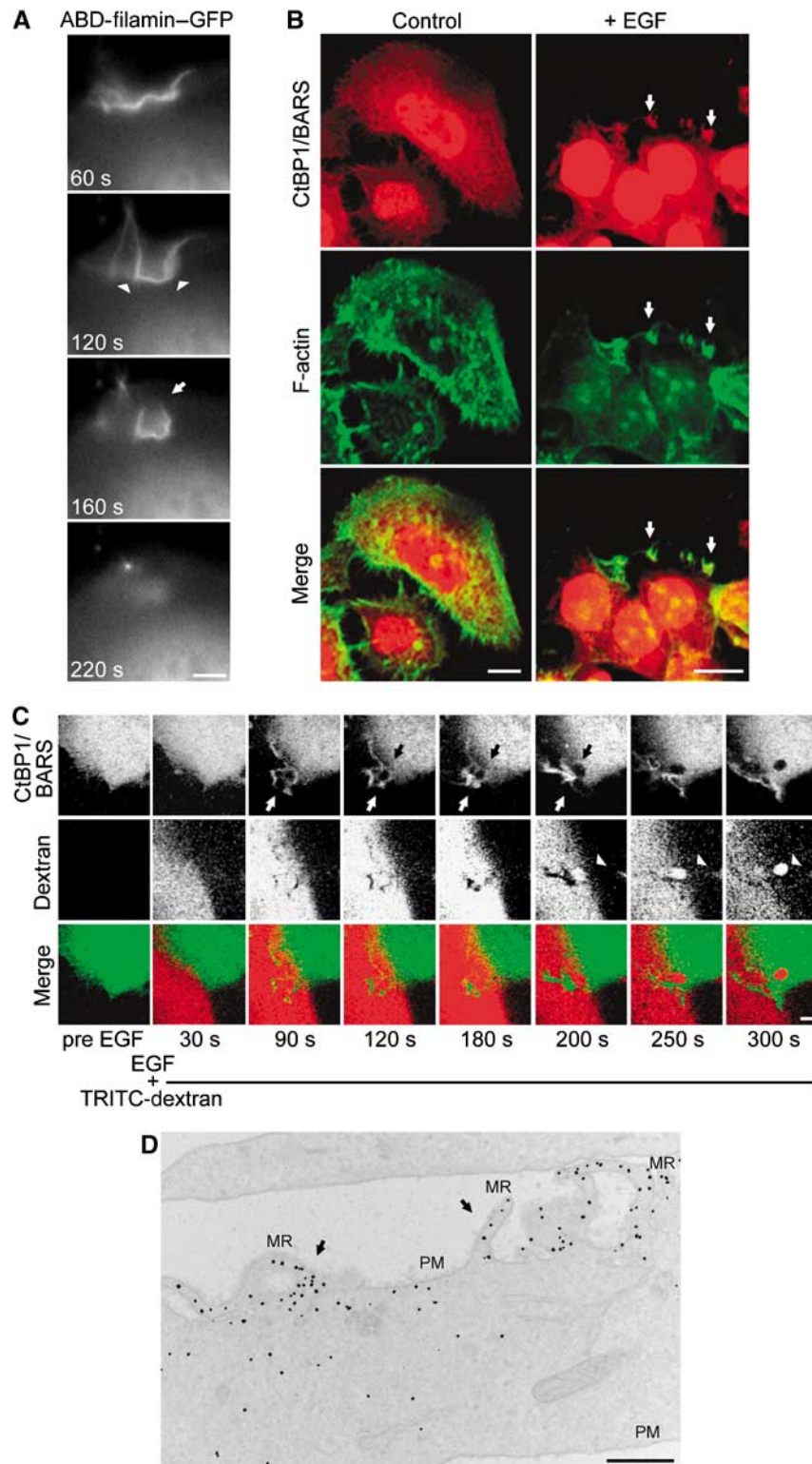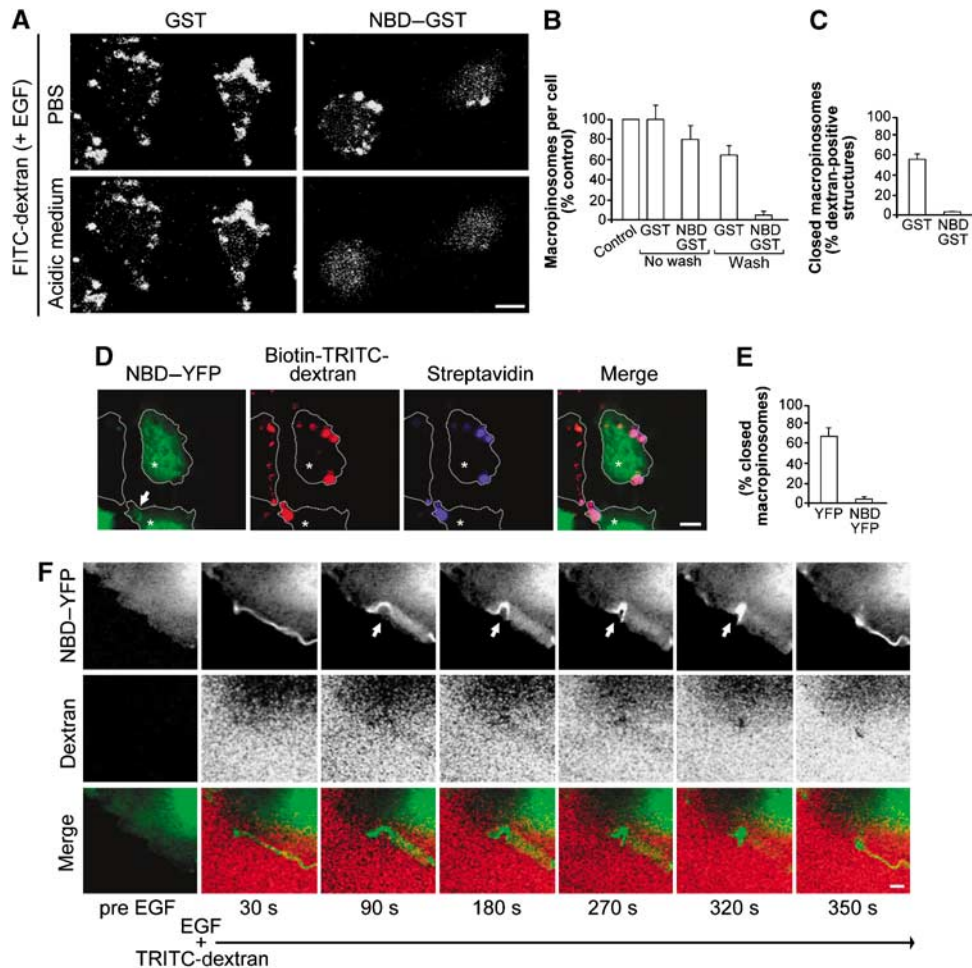
Figure 3 Characterization of the role of CtBP1/BARS in macropinosome formation in A431 cells. (**A**) Cells were microinjected with GST or NBD–GST, as indicated, and incubated for 1 h in serum-free Ringer's buffer and for 8 min in Ringer's buffer containing 50 ng/ml EGF and FITC-conjugated dextran. The cells were then fixed without the pre-fixing wash, to detect both fully incorporated macropinosomes and formed macropinocytic cups still connected with the plasma membrane. To distinguish between these, the fixed cells were incubated in PBS at either neutral pH (PBS) or pH 5 (acidic medium), to quench fluorescence of the macropinosomes connected with the plasma membrane. The time frame of our confocal analysis is less than 10 min. (**B, C**) Quantification of macropinosomes in cells without or with the pre-fixing wash (B) and of closed macropinosomes (C), in cells treated as in (A), as indicated (see Materials and methods). (**D**) Cells were transfected with NBD–YFP (6 h overexpression) and incubated for 1 h in serum-free Ringer's buffer and for 8 min in Ringer's buffer containing 50 ng/ml EGF and TRITC- and biotin-conjugated dextran. The cells were then fixed without the pre-fixing wash, as indicated in (A). To distinguish between fully incorporated and still connected macropinosomes, the fixed cells were stained (without permeabilization) with streptavidin-633 (to reveal the latter). Arrow, NBD-YFP at the macropinocytic cup. (**E**) Quantification of closed macropinosomes in cells transfected with YFP or NBD–YFP and treated as in (D). (**F**) Cells were transfected with NBD–YFP (6 h of overexpression), incubated for 1 h in serum-free Ringer's buffer and then with 50 ng/ml EGF and TRITC-labelled dextran. Representative frames of time-lapse imaging for NBD–YFP (green) and TRITC-dextran (red) and merged signals are shown, as indicated. Upper panels, 90–320 s: arrows, macropinosomes not yet sealed. More than 50 cells were analysed under each experimental condition and the data are means ± s.d. from three independent experiments. Scale bars: (A, D) 10 μm; (F) 1 μm.

Figure 2 Effects of EGF stimulation on CtBP1/BARS localization in A431 cells. (**A**) Cells were transfected with the actin-binding domain of filamin–GFP (ABD-filamin–GFP), incubated for 1 h in serum-free Ringer's buffer and stimulated with 50 ng/ml EGF. Representative frames of time-lapse imaging for ABD-filamin–GFP are shown. Arrowheads, cup-shaped macropinocytic invaginations; arrow, closing macropinocytic cup. (**B**) Immunofluorescence analyses of endogenous CtBP1/BARS and F-actin localization in cells incubated for 1 h in serum-free Ringer's buffer and then for 8 min in Ringer's buffer in the absence (control) or presence (+) of 50 ng/ml EGF. The cells were then fixed and stained with the p50-2 anti-CtBP1/BARS antibody (red) and 488-conjugated phalloidin to reveal actin organization (F-actin), as indicated. The merged signals are shown in the lower panels. White arrows, macropinocytic cups seen among plasma membrane ruffles. (**C**) Cells were transfected with CtBP1-S/BARS–YFP (6 h of overexpression), incubated for 1 h in serum-free Ringer's buffer and stimulated with 50 ng/ml EGF in the presence of TRITC-conjugated dextran. Representative frames of time-lapse imaging for CtBP1-S/BARS–YFP (green) and TRITC-dextran (red) and merged signals are shown, as indicated. Upper panels, 90–200 s: white arrow, closing macropinocytic cup and CtBP1-S/BARS enrichment at the neck; black arrow, disappearance of CtBP1-S/BARS–YFP from the base of the macropinocytic cup. Middle panels, 200–300 s: arrowhead, internalized macropinosome. (**D**) Immuno-EM analysis of CtBP1-S/BARS–YFP localization in cells prepared and stimulated with 50 ng/ml EGF for 8 min, as in (A). The cells were then fixed, stained with an anti-YFP antibody and prepared for EM (see Materials and methods). MR, membrane ruffles; PM, plasma membrane. Black dots, enrichment of CtBP1-S/BARS–YFP at plasma membrane ruffles (arrows). More than 50 cells were analysed under each experimental condition, in three independent experiments. Scale bars: (A, C) 1 μm; (B) 10 μm; (D) 600 nm.
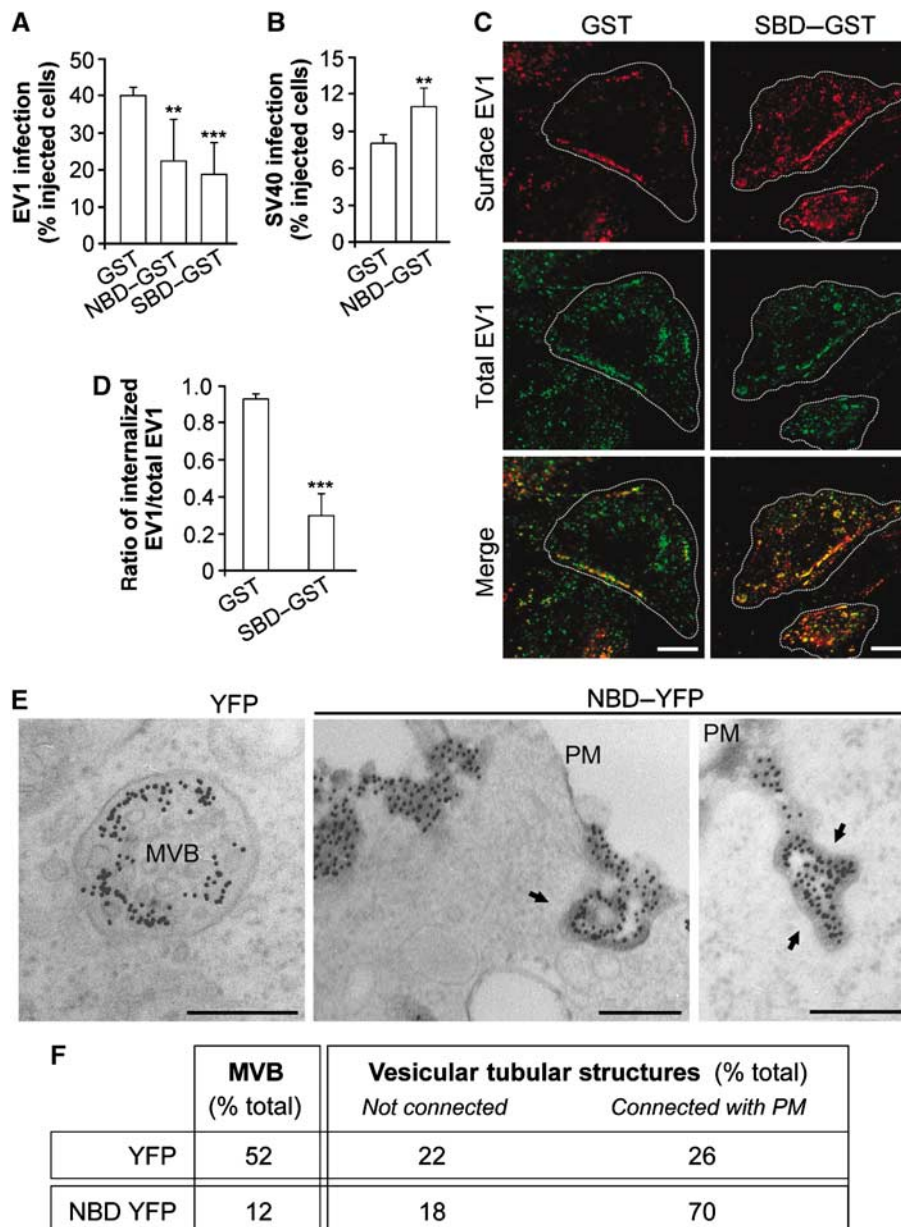
Figure 4 Effects of CtBP1/BARS inhibition on infection and $\alpha_2\beta_1$-mediated internalization of EV1 in SAOS cells. (**A**) Cells were microinjected with GST, NBD–GST or SBD–GST, as indicated, incubated with EV1 virus for 6 h and then fixed and quantified for EV1-infected cells (see Materials and methods). (**B**) As (A), with SV40 virus for 12 h, as indicated, for SV40-infected cells. (**C**) As (A), with EV1 virus for 2 h, as indicated. Cells were fixed and labelled for surface-bound (red) and total (green) EV1 (with non-permeabilized and permeabilized cells, respectively), with merged signal shown. Green dots in the merged signal represent internalized virus. (**D**) Quantification of the ratio of internalized to total EV1, as described in (C). More than 100 cells were analysed under each experimental condition, and the data are means ± s.e. from three independent experiments. (**E**) Cells were transfected with empty YFP vector or NBD–YFP for 2 h, as indicated, then incubated for 2 h with an anti-α_2-integrin antibody to induce integrin internalization and fixed and prepared for EM. Integrin was revealed with a gold-conjugated secondary antibody, and membranes accessible by extracellular medium were revealed by treatment with ruthenium red (electron-dense membranes). Left-hand panel, multivesicular body (MVB) in control cells. Centre and right-hand panels, integrin-labelled vesicular-tubular structures connected with the plasma membrane (PM). Arrows, electron-dense membranes. (**F**) Quantification from morphometric analysis of cells treated as in (E), showing per cent distributions of integrin-labelled membranes among the not connected/connected phenotypes, corrected for transfection efficiency (40%). Altogether 700 structures were counted under each condition. Scale bars: (C) 10 μm; (E) 200 nm. **$P < 0.005$, ***$P < 0.001$ (Student's t-test).

pathway, namely SV40, a well-characterized virus that uses caveolae to infect CV-1 cells (Pelkmans et al, 2001). Here, SV40 infection was not inhibited; rather, it was slightly enhanced by expression of the CtBP1/BARS DN NBD mutant, possibly as a consequence of upregulation of the caveolar entry route secondary to the block of macropino-cytosis (Damke et al, 1995) (Figure 4B). This indicates that

CtBP1/BARS controls the macropinocytic entry route specifically, rather than the infection process in general.

Finally, we examined the internalization of $\alpha_2\beta_1$ integrins upon clustering using a gold-conjugated anti-$\alpha 2$-integrin antibody, a process that closely mimics EV1 internalization (Upla et al, 2004) and that can be monitored by EM (through visualization of the conjugated gold). After stimulating inter-

nalization with this anti-α2-integrin antibody, we stained the plasma membrane with the membrane-impermeant marker ruthenium red and processed the cells for EM. Using this approach, if an invaginated integrin container does not undergo fission, it will be stained with ruthenium red. After addition of the antibody and integrin clustering, the internalized integrins were initially seen within simple tubulo-vacuolar structures and then later inside large multivesicular bodies (Karjalainen et al, 2008; Figure 4E). At this later time (2 h), the vast majority of the internalized integrin containers were not labelled with ruthenium red in control cells (i.e., the integrins were in fully 'sealed' tubulo-vacuolar macropinocytic structures or multivesicular bodies) (Figure 4E and F). In contrast, in cells transfected with the DN mutant NBD, most of the integrins were still present in surface-bound invaginations (ruthenium red labelled; Figure 4E, arrow), presumably representing non-sealed macropinocytic cups (Figure 4E and F), and indicating that most of the cups in these cells had not undergone fission. Notably, these structures are smaller than the macropinosomes seen in A431 cells. Nevertheless, the fact that they share their underlying machinery (Karjalainen et al, 2008) with classical macropinocytic processes indicates that they are macropinosome in nature. The differences in macropinosome size between SAOS and A431 cells might be due to the different stimuli used to trigger the internalization or due to differences between these cell types.

Collectively, these data indicate that CtBP1/BARS is required for macropinocytosis at the fissioning stage. They also demonstrate a role for CtBP1/BARS in EV1 infection. In this regard, it is of note that also adenovirus 3 is internalized via CtBP1/BARS-dependent macropinocytosis (Amstutz et al, 2008), indicating that this endocytic pathway might be a common viral entry route.

Pak1-mediated CtBP1/BARS phosphorylation is required for fission of the macropinocytic cup

Finally, we examined the mechanisms of activation of CtBP1/ BARS in EGF-receptor-mediated macropinocytosis. Among the components of the EGF signalling pathway, the kinase Pak1 is a likely candidate for a CtBP1/BARS activator. Pak1 is activated by the EGF receptor and is required for EGF-induced actin reorganization and macropinocytosis (Dharmawardhane et al, 1997, 2000). Moreover, Pak1 interacts directly with CtBP1-L/BARS, and following EGF stimulation, it phosphorylates CtBP1-L/BARS in vivo on serine 158 (serine 147 in CtBP1-S/BARS) (Barnes et al, 2003). This phosphorylation triggers the redistribution of CtBP1/BARS from the nucleus to the cytoplasm and inhibits the CtBP1-L/ BARS nuclear co-repressor activity (Barnes et al, 2003).

To investigate the role of CtBP1/BARS phosphorylation by Pak1 in macropinosome fission, we first sought to confirm the role of Pak1 in EGF-induced membrane ruffling and macropinocytosis under our conditions, by transfecting A431 cells with the Pak1 auto-inhibitory domain (an established tool to inhibit endogenous Pak1; Dharmawardhane et al, 2000) and by treating the cells with siRNAs against Pak1 (Delorme et al, 2007). Indeed, the macropinocytic response to EGF was prevented here, confirming the role of Pak1 in this reaction (Figure 5A and B). We also examined the localization of Pak1 upon addition of EGF. Again, in agreement with a previous report (Dharmawardhane et al, 1997), Pak1 was

recruited from the cytosol onto plasma membrane ruffles, where it colocalized with CtBP1/BARS (Figure 5C). We then examined whether CtBP1/BARS was phosphorylated in vivo under the same conditions. Indeed EGF induced a rapid three-fold increase in the levels of CtBP1/BARS phosphorylation; moreover, CtBP1/BARS was efficiently phosphorylated by Pak1 in vitro; see Supplementary Figure 2A and B.

Next, we generated two CtBP1-S/BARS point mutants in which the critical serine in position 147 was replaced by either alanine (S147A, as 'phospho-depleted') or aspartic acid (S147D, as 'phospho-mimetic'). In quiescent cells, the localization of both of these CtBP1-S/BARS mutants was both nuclear and cytosolic; however, the phospho-depleted mutant localized predominantly to the nucleus, whereas the phospho-mimetic mutant localized mostly to the cytosol, as expected (Barnes et al, 2003) (Supplementary Figure 2C). After EGF stimulation, both of these CtBP1-S/BARS mutants were found at plasma membrane ruffles (Figure 6A), indicating that plasma membrane recruitment of CtBP1/BARS is independent of its phosphorylation by Pak1. Of note, given the increasingly recognized role of actin in membrane fission, the mechanism of this recruitment is an interesting question for future studies.

We then examined the effects of these mutants in macropinocytosis by microinjecting them into A431 cells. The phospho-depleted mutant strongly inhibited macropinocytosis (i.e., it behaved as a DN; Figure 6B and C); instead, the phospho-mimetic CtBP1-S/BARS had no apparent effect (Figure 6B and C). Neither mutant affected actin ruffling (Figure 6A). We then tested if the block of macropinocytosis induced by the phospho-depleted mutant can be reversed by the phospho-mimetic mutant (or by wild-type CtBP1-S/ BARS), by co-injecting the former mutant along with the latter. As shown in Figure 6D, the phospho-mimetic mutant completely restored the inhibited macropinocytic response even at low molar ratios (mimetic over depleted), whereas co-injecting wild-type CtBP1/BARS induced only a partial recovery of macropinocytosis at high molar ratios. These data thus suggest that the phospho-mimetic mutant is more active than wild-type CtBP1/BARS and may, in fact, function as a constitutively active CtBP1/BARS. It is also formally possible, albeit unlikely, that the phospho-mimetic mutant prevents the inhibitory effect of the phospho-depleted mutant by dimerizing with it efficiently and somehow sequestering it from the fission reaction. Regardless of this distinction, these collective results indicate that phosphorylation of CtBP1/ BARS by Pak1 is necessary for EGF-receptor-activated macropinocytosis.

Discussion

In this study, we show that the protein CtBP1/BARS is required for the fission of the macropinosome neck during EGF-mediated macropinocytosis, and we analyse the mechanisms leading to CtBP1/BARS activation in this process. Thus, we find that upon EGF receptor engagement, CtBP1/ BARS is translocated to the macropinocytic cup and its surrounding membrane. Moreover, at the same time, CtBP1/BARS is phosphorylated, and its phosphorylation on a specific serine that is known to be a Pak1 substrate is necessary for the fission of the macropinocytic cup.
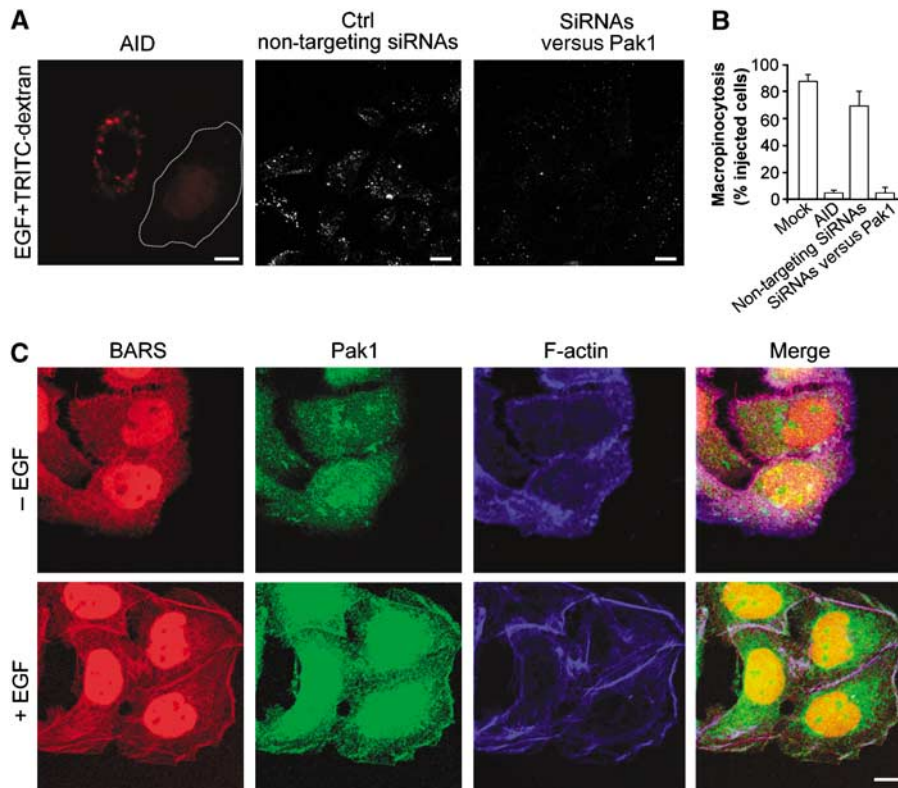
Figure 5 Effects of the Pak1 auto-inhibitory domain on EGF-stimulated macropinocytosis and localization of endogenous Pak1 and CtBP1/BARS in A431 cells. (**A**) Cells were transfected with the Pak1 auto-inhibitory domain (AID) for 12 h or for 48 h with non-targeting siRNAs or siRNAs targeted to Pak1, incubated for 1 h in serum-free Ringer's buffer and then for 8 min in Ringer's buffer with 50 ng/ml EGF and TRITC-conjugated dextran. After fixing, the cells were examined under confocal microscopy for macropinocytosis. (**B**) Quantification of macro-pinocytosing cells treated as in (A), as indicated (see Materials and methods). (**C**) Immunofluorescence analyses of endogenous CtBP1/BARS, Pak1 and F-actin localization. Cells were incubated for 1 h in serum-free Ringer's buffer and for 8 min in Ringer's buffer in the absence (−) or presence (+) of 50 ng/ml EGF. Then the cells were fixed and stained with the p50-2 anti-CtBP1/BARS antibody (BARS; red), an anti-Pak1 antibody (Pak1; green) and 633-conjugated phalloidin, to reveal actin organization (F-actin; blue); the merged signals are also shown. Scale bars: (A, C) 10 μm.

These conclusions rest on the following lines of evidence: (a) upon EGF stimulation, CtBP1/BARS is recruited to membrane ruffles and to forming macropinocytic cups, as shown by immunofluorescence, EM and time-lapse imaging; (b) fission of the EGF-stimulated macropinosomes can be inhibited by a variety of treatments that block CtBP1/BARS activity; and (c) CtBP1/BARS is phosphorylated during macropinocytosis, and the microinjection of a CtBP1-S/BARS point mutant in which a serine that is known to be a phosphorylation substrate of Pak1 was replaced by alanine (S147A, as 'phospho-depleted') was able to strongly inhibit macropinocytosis (i.e., it behaved as a DN), whereas the mutant in which the serine was replaced by aspartic acid (S147D, as 'phospho-mimetic') potently reversed this inhibition.

Placed in the context of our current understanding of macropinocytosis, our findings suggest the following scheme: the EGF (or other) receptor initiates a complex signalling cascade that, among other effects, leads to the recruitment of Rac to the plasma membrane (Swanson and Watts, 1995; Amyere *et al*, 2002; Falcone *et al*, 2006), which recruits and activates Pak1 (Dharmawardhane *et al*, 2000). This kinase stimulates actin polymerization via the LIMK1–cofilin pathway, which in turn leads to the formation of membrane ruffles and of the macropinocytic cup (Edwards *et al*, 1999). Pak1 also binds the SBD domain of CtBP1/BARS

through its auto-inhibitory portion (our unpublished data; Barnes *et al*, 2003) and phosphorylates the CtBP1/BARS NBD domain. The activated phospho-CtBP1/BARS is essential for the fissioning machinery that closes the cup. Importantly, a similar sequence of events appears to apply also to the macropinocytosis-mediated entry of some viruses (this study; Amstutz *et al*, 2008; Karjalainen *et al*, 2008), a process that is obviously relevant to human pathology. Incidentally, as CtBP1/BARS binds to Pak1 via its SBD domain, this offers a possible explanation for the inhibitory effect of this domain (the SBD mutant) on macropinocytosis (it competes with CtBP1/BARS for binding to Pak1) and, at the same time, of why SBD does not inhibit cargo exit from the Golgi (this traffic step does not involve Pak1; our unpublished results).

With respect to the molecular mechanisms of CtBP1/BARS-dependent fission, the insight gained in this study opens interesting avenues for future developments. On a speculative note, from free energy calculations based on molecular dynamics simulations of non-phosphorylated and phosphorylated CtBP1-S/BARS, the phosphorylation of CtBP1/BARS by Pak1 can be predicted to induce a reduced stability of the dimeric conformation (CtBP1/BARS crystallizes as a dimer; Nardini *et al*, 2003) in favour of a monomeric state (this study; see Supplementary Figure 3 and Supplementary data). This is of interest because a similar dimer–monomer shift has been proposed to be induced by

the binding to CtBP1/BARS of the acyl-CoA cofactor that is involved in the fission of COPI-coated vesicles (Glick and Rothman, 1987; Nardini et al, 2003; Yang et al, 2005). It is thus possible that Pak1-dependent phosphorylation and acyl-CoA binding act synergistically to generate a monomeric form of CtBP1/BARS. Monomers might facilitate fissioning either by binding new partners in an assembling fission complex or by exposing hydrophobic residues that might then participate directly in the final destabilization of the macropinosome neck (Yang et al, 2005).

With regard to experimental developments, this study defines the S147A and the S147D CtBP1/BARS single point mutants as being DN and constitutively active proteins in fission, respectively. These mutants should thus provide the means for the identification of differential CtBP1/BARS interactors in membrane fission, in analogy with similar studies based on using active/inactive GTPase mutant couples to identify GTPase effectors (Christoforidis and Zerial, 2000).

Another important facet of this study concerns the relationship between the two apparently unrelated functions of CtBP1/BARS, one in macropinocytosis (and further trafficking steps) and the other as a transcriptional co-repressor. CtBP1/BARS is one of the many known bifunctional proteins that shuttle between the cytoplasm and the nucleus in their control of both cytosolic functions and gene expression (Vecchi et al, 2001; Hervy et al, 2006). The current data now suggest that the phosphorylation of CtBP1/BARS by Pak1 is a mechanistic link between these two activities of CtBP1/BARS, insofar as Pak1 switches CtBP1/BARS on for membrane fission and at the same time turns it off as a co-repressor (Barnes et al, 2003). This provides a potential lead to understand how cells coordinate their trafficking with other functions across separate compartments.

Materials and methods

Reagents

GST–CtBP1-S/BARS, GST–SBD and GST–NBD were expressed and purified as described previously (Hidalgo Carcedo et al, 2004; Bonazzi et al, 2005). DNA coding for GST–CtBP1/BARS (S147A) and GST–CtBP1/BARS (S147D) was generated using the Quik-Change Site-Directed Mutagenesis Kit (Stratagene, La Jolla, CA) with the following pair of oligonucleotides: CtBP1/BARS(S147A) 5′-GCACTCGGGTCCAGGCTGTAGAGCAGATCC-3′ and 5′-GGATCTGC TCTACAGCCTGGACCCGAGTGC-3′; CtBP1/BARS(S147D) 5′-GCACT CGGGTCCAGGATGTAGAGCAGATCC-3′ and 5′-GGATCTGCTCTACAT CCTGGACCCGAGTGC-3′.

The CtBP1/BARS mutants were verified by DNA sequencing and purified as described previously for CtBP1-S/BARS (Bonazzi et al, 2005). The p50-2 anti-CtBP1/BARS rabbit polyclonal antibody was raised against GST–CtBP1-S/BARS and purified by affinity chromatography, as described previously (Bonazzi et al, 2005). The Pak1-AID construct was provided by Ed Manser (Institute of Molecular and Cell Biology, Singapore). The anti-Pak1 polyclonal antibody was obtained from Transduction Laboratories (Lexington, KY). The conjugated phalloidin (488, 546, 633) was obtained from Sigma (St Louis, MO). The mouse monoclonal antibody to GFP was from Abcam (Cambridge, UK). The secondary antibody Alexa 488 and 546 were obtained from Molecular Probes (Eugene, OR). The nanogold-conjugated Fab fragments of anti-rabbit IgG and Gold Enhancer were from Nanoprobes (NY, USA). The siRNAs were from Dharmacon (Lafayette, CA, USA; catalogue number M-008609-01).
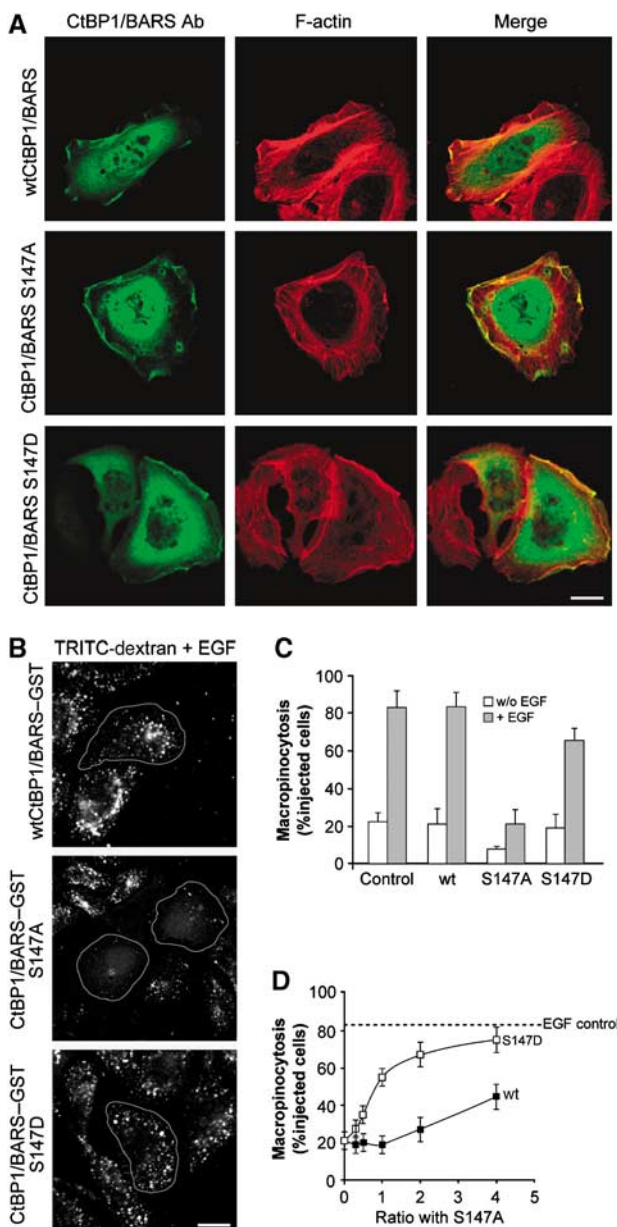

Figure 6 Characterization of Pak1-mediated CtBP1/BARS phosphorylation during macropinocytosis in A431 cells. (**A**) Immunofluorescence localization of wild-type (wt) CtBP/BARS and its S147A and S147D mutants and F-actin in EGF-stimulated cells. Cells were transfected for 6 h with the indicated CtBP1/BARS constructs, incubated for 1 h in serum-free Ringer's buffer and then for 8 min in Ringer's buffer with 50 ng/ml EGF. The cells were then fixed and stained with the p50-2 anti-CtBP1/BARS antibody (BARS Ab; green) and 546-conjugated phalloidin to reveal actin organization (F-actin; red); the merged signals are also shown. (**B**) Cells were microinjected with wild-type (wt) CtBP1-S/BARS–GST or its phospho-mimetic (S147D-BARS–GST) and phospho-depleted (S147A-BARS–GST) mutants, incubated for 1 h in serum-free Ringer's buffer and for 8 min in Ringer's buffer containing 50 ng/ml EGF and TRITC-conjugated dextran. (**C**) Quantification of macropinocytosing cells treated as in (B), as indicated (see Materials and methods). (**D**) Cells were microinjected with different molar ratios of wild-type CtBP1-S/BARS–GST (wt) or CtBP1-S/BARS-S147D mutant (S147D), both versus CtBP1-S/BARS-S147A, incubated for 1 h in serum-free Ringer's buffer and for 8 min in Ringer's buffer containing 50 ng/ml EGF and TRITC-conjugated dextran. Quantification for macropinocytosing cells was carried out, with more than 100 cells analysed under each experimental condition. Dashed line, EGF-stimulated control macropinocytosis. Data are means ± s.d. from three independent experiments. Scale bars: (A, B) 10 μm.

Macropinocytosis assays

A431 cells were maintained in DMEM containing 10% fetal bovine serum. The cells were plated on coverslips in 24-well plates and cultured for 2 days to a confluency of 80%. Before experiments, the cells were incubated for 1 h at 37°C in serum-free Ringer's buffer (155 mM NaCl, 5 mM KCl, 1 mM MgCl$_2$, 2 mM Na$_2$HPO$_4$, 10 mM glucose, 10 mM HEPES, pH 7.2, 0.5 mg/ml BSA). The serum-starved cells were stimulated with 50 ng/ml EGF (Sigma). To detect the newly formed macropinosomes, this stimulation was performed in the presence of 1 mg/ml FITC- or TRITC-labelled, lysine-fixable dextran (Molecular Probes, Eugene, OR), as probes of fluid-phase macropinocytosis, in Ringer's buffer. The cells were then washed to remove the unbound dextran, fixed with 4% paraformaldehyde and either monitored by confocal fluorescence microscopy or further processed for immunofluorescence microscopy (Zeiss LSM510 META confocal microscope system (Carl Zeiss, Gottingen, Germany), objective: × 63, 1.4 NA oil, acquisition LSM510, software: LSM 510 (3.2)). Cells showing ⩾10 dextran-positive structures were considered to be macropinocytosing and were scored positive for macropinocytosis. The levels of macropinocytosis are given as percentages of the total cells in this scoring category. All of the data are means ± s.d. deriving from at least 100 cells/determination. Each experiment was repeated at least three times. The immuno-fluorescence analyses were performed as described previously (Bonazzi *et al*, 2005).

Transfection and live-cell imaging

The cells were transfected with CtBP1-S/BARS–YFP or ABD-filamin–GFP 6 h before the experiments, using Transfast reagents (Promega). Following EGF stimulation, the effects of these transfections were followed by live-cell imaging under a confocal laser microscope (Zeiss LSM510 META confocal microscope system (Carl Zeiss, Gottingen, Germany), objective: × 63, 1.4 NA oil, acquisition LSM510, software: LSM 510 (3.2)) in Ringer's buffer at 37°C.

Differential staining of surface versus intracellular antigens

EV1 treatment and α2β1 integrin clustering were carried out as described previously (Upla *et al*, 2004). The differential staining of EV1 was by sequential labelling of EV1 before and after permeabilization using differently fluorescent secondary antibodies (Upla *et al*, 2004). α2β1 integrin clusterin 8 was induced by a fluorescent secondary antibody and, after fixing, the surface-bound integrin was stained with another secondary antibody conjugated to a different colour. Quantification of these ratios was performed using the free open-source software BioimageXD (http://www.bioimgexd.net). We added to this software an advanced colocalization tool and a simple algorithm for calculating the relative colocalization, as the ratio [channel 2]/([channel 1]−[co-localization]), where channel 1 is the voxels stained before permeabilization, channel 2 the voxels stained after permeabilization and the colocalization the voxels with channels 1 and 2 colocalization. Only the voxels above a set threshold value were included in the quantification (with a threshold of 130 for 8-bit data), to avoid counting diffuse background staining.

Microinjection

For each experiment, about 200 A431 or SAOS (α2β1) cells were microinjected with the purified proteins at concentrations of 2–3 mg/ml in microinjection buffer (10 mM NaH$_2$PO$_4$/Na$_2$HPO$_4$, pH 7.4, 70 mM KCl). Prior to injection, the proteins were mixed with 0.4 mg/ml FITC- or TRITC-labelled dextran (Molecular Probes) as tracers of microinjection. The proteins were microinjected 1 h before the macropinocytosis or the infection assays. With CtBP1/ BARS, this should increase its endogenous concentration by some 5- to 15-fold, based on the observations that the intracellular concentration of CtBP1/BARS is 20 ng/ml (our unpublished data) and on the assumption that 5–10% of the cell volume was injected. The p50-2 anti-CtBP1/BARS antibody was injected at 2 mg/ml 1 h before further experimental procedures.

Transfection with siRNAs

A431 cells were transfected for 72 h with a Smart Pool of siRNA sequences (CCGUCAAGCAGAUGAGACAUU; GGAUAGAGACCAC GCCAGUUU; GCUCGCACUUGCUCAACAAUU; GAGCAGGCAU CCAUCGAGAUU; Dharmacon) directed against CtBP1/BARS using oligofectamine (Invitrogen, Carlsbad, CA, USA), according to the manufacturer's instructions. Mock transfection and transfection of non-targeting siRNA sequences (Dharmacon) were used as controls. After transfection, the intracellular protein contents were assessed by SDS–PAGE and the cells were further processed according to the experimental procedures.

Electron microscopy

A431 cells were microinjected with BARS–YFP (6 h of overexpression) before the macropinocytosis assay. Fixation and immuno-gold detection of the YFP tag for EM was performed using an antibody to GFP, as previously described (Polishchuk *et al*, 2000). After immunolabelling, cells were embedded in Epon-812 and cut into thin sections.

SAOS-α2β1 cells were first transfected with control YFP or NBD–YFP plasmids for 2 days. To visualize α2β1 integrin under EM, it was clustered by sequential treatment of a primary antibody (anti-Has6, from Fiona M Watt, Cancer Research, London, UK) and a secondary rabbit anti-mouse IgG antibody (Sigma) on ice (Upla *et al*, 2004). The cells were then treated with protein A gold (10 nm; G Posthuma and J Slot, University Medical Centre Utrecht, The Netherlands) on ice, followed by a further incubation for 2 h at 37°C. The cells were finally washed in cacodylate buffer, pH 7.3, and stained with 1.3% glutaraldehyde and 0.07 mg/ml ruthenium red in cacodylate buffer at room temperature for 1 h. The cells were then post-fixed in 1.7% osmium tetroxide containing 0.07 mg/ml ruthenium red and dehydrated and treated for EM following epon embedding, as described previously (Upla *et al*, 2004).

Supplementary data

Supplementary data are available at *The EMBO Journal* Online (http://www.embojournal.org).

References

Ahram M, Sameni M, Qiu RG, Linebaugh B, Kirn D, Sloane BF (2000) Rac1-induced endocytosis is associated with intracellular proteolysis during migration through a three-dimensional matrix. *Exp Cell Res* **260:** 292–303

Amstutz B, Gastaldelli M, Kälin S, Imelli N, Boucke K, Wandeler E, Mercer J, Hemmi S, Greber UF (2008) Subversion of CtBP1-controlled macropinocytosis by human adenovirus serotype 3. *EMBO J* (submitted), advance online publication 6 March 2008; doi:10.1038/emboj.2008.38

Amyere M, Mettlen M, Van Der Smissen P, Platek A, Payrastre B, Veithen A, Courtoy PJ (2002) Origin, originality, functions, subversions and molecular signalling of macropinocytosis. *Int J Med Microbiol* **291:** 487–494

Barnes CJ, Vadlamudi RK, Mishra SK, Jacobson RH, Li F, Kumar R (2003) Functional inactivation of a transcriptional corepressor by a signaling kinase. *Nat Struct Biol* **10:** 622–628

Bonazzi M, Spano S, Turacchio G, Cericola C, Valente C, Colanzi A, Kweon HS, Hsu VW, Polishchuk EV, Polishchuck RS, Sallese M,

Pulvirenti T, Corda D, Luini A (2005) CtBP3/BARS drives membrane fission in dynamin-independent transport pathways. *Nat Cell Biol* **7:** 570–580

Chinnadurai G (2002) CtBP, an unconventional transcriptional corepressor in development and oncogenesis. *Mol Cell* **9:** 213–224

Chinnadurai G (2003) CtBP family proteins: more than transcriptional corepressors. *BioEssays* **25:** 9–12

Christoforidis S, Zerial M (2000) Purification and identification of novel Rab effectors using affinity chromatography. *Methods* **20:** 403–410

Colanzi A, Carcedo CH, Persico A, Cericola C, Turacchio G, Bonazzi M, Luini A, Corda D (2007) The Golgi mitotic checkpoint is controlled by BARS-dependent fission of the Golgi ribbon into separate stacks in G2. *EMBO J* **26:** 2465–2476

Conner SD, Schmid SL (2003) Regulated portals of entry into the cell. *Nature* **422:** 37–44

Corda D, Colanzi A, Luini A (2006) The multiple activities of CtBP/BARS proteins: the Golgi view. *Trends Cell Biol* **16:** 167–173

Damke H, Baba T, van der Bliek AM, Schmid SL (1995) Clathrin-independent pinocytosis is induced in cells overexpressing a temperature-sensitive mutant of dynamin. *J Cell Biol* **131:** 69–80

Delorme V, Machacek M, Dermardirossian C, Anderson KL, Wittmann T, Hanein D, Waterman-Storer C, Danuser G, Bokoch GM (2007) Cofilin activity downstream of pak1 regulates cell protrusion efficiency by organizing lamellipodium and lamella actin networks. *Dev Cell* **13:** 646–662

Dharmawardhane S, Sanders LC, Martin SS, Daniels RH, Bokoch GM (1997) Localization of p21-activated kinase 1 (PAK1) to pinocytic vesicles and cortical actin structures in stimulated cells. *J Cell Biol* **138:** 1265–1278

Dharmawardhane S, Schurmann A, Sells MA, Chernoff J, Schmid SL, Bokoch GM (2000) Regulation of macropinocytosis by p21-activated kinase-1. *Mol Biol Cell* **11:** 3341–3352

Edwards DC, Sanders LC, Bokoch GM, Gill GN (1999) Activation of LIM-kinase by Pak1 couples Rac/Cdc42 GTPase signalling to actin cytoskeletal dynamics. *Nat Cell Biol* **1:** 253–259

Falcone S, Cocucci E, Podini P, Kirchhausen T, Clementi E, Meldolesi J (2006) Macropinocytosis: regulated coordination of endocytic and exocytic membrane traffic events. *J Cell Sci* **119:** 4758–4769

Ferguson SM, Brasnjo G, Hayashi M, Wolfel M, Collesi C, Giovedi S, Raimondi A, Gong LW, Ariel P, Paradise S, O'Toole E, Flavell R, Cremona O, Miesenbock G, Ryan TA, De Camilli P (2007) A selective activity-dependent requirement for dynamin 1 in synaptic vesicle endocytosis. *Science* **316:** 570–574

Glebov OO, Bright NA, Nichols BJ (2006) Flotillin-1 defines a clathrin-independent endocytic pathway in mammalian cells. *Nat Cell Biol* **8:** 46–54

Glick BS, Rothman JE (1987) Possible role for fatty acyl-coenzyme A in intracellular protein transport. *Nature* **326:** 309–312

Grist NR, Bell EJ, Assaad F (1978) Enteroviruses in human disease. *Prog Med Virol* **24:** 114–157

Grooteclaes M, Deveraux Q, Hildebrand J, Zhang Q, Goodman RH, Frisch SM (2003) C-terminal-binding protein corepresses epithelial and proapoptotic gene expression programs. *Proc Natl Acad Sci USA* **100:** 4568–4573

Haigler HT, McKanna JA, Cohen S (1979) Rapid stimulation of pinocytosis in human carcinoma cells A-431 by epidermal growth factor. *J Cell Biol* **83:** 82–90

Hamasaki M, Araki N, Hatae T (2004) Association of early endosomal autoantigen 1 with macropinocytosis in EGF-stimulated A431 cells. *Anat Rec A Discov Mol Cell Evol Biol* **277:** 298–306

Hervy M, Hoffman L, Beckerle MC (2006) From the membrane to the nucleus and back again: bifunctional focal adhesion proteins. *Curr Opin Cell Biol* **18:** 524–532

Hewlett LJ, Prescott AR, Watts C (1994) The coated pit and macropinocytic pathways serve distinct endosome populations. *J Cell Biol* **124:** 689–703

Hidalgo Carcedo C, Bonazzi M, Spano S, Turacchio G, Colanzi A, Luini A, Corda D (2004) Mitotic Golgi partitioning is driven by the membrane-fissioning protein CtBP3/BARS. *Science* **305:** 93–96

Karjalainen M, Kakkonen E, Upla P, Paloranta H, Kankaanpää P, Liberali P, Renkema GH, Hyypiä T, Heino J, Marjomäki V (2008) A raft-derived, Pak1-regulated entry participates in a2b1 integrin-dependent sorting to caveosomes. *Mol Biol Cell* (submitted)

Kirkham M, Parton RG (2005) Clathrin-independent endocytosis: new insights into caveolae and non-caveolar lipid raft carriers. *Biochim Biophys Acta* **1746:** 349–363

Lee E, Knecht DA (2002) Visualization of actin dynamics during macropinocytosis and exocytosis. *Traffic* **3:** 186–192

McNiven MA, Thompson HM (2006) Vesicle formation at the plasma membrane and *trans*-Golgi network: the same but different. *Science* **313:** 1591–1594

Meier O, Boucke K, Hammer SV, Keller S, Stidwill RP, Hemmi S, Greber UF (2002) Adenovirus triggers macropinocytosis and endosomal leakage together with its clathrin-mediated uptake. *J Cell Biol* **158:** 1119–1131

Mellstrom K, Heldin CH, Westermark B (1988) Induction of circular membrane ruffling on human fibroblasts by platelet-derived growth factor. *Exp Cell Res* **177:** 347–359

Nardini M, Spano S, Cericola C, Pesce A, Massaro A, Millo E, Luini A, Corda D, Bolognesi M (2003) CtBP/BARS: a dual-function protein involved in transcription co-repression and Golgi membrane fission. *EMBO J* **22:** 3122–3130

Newton AJ, Kirchhausen T, Murthy VN (2006) Inhibition of dynamin completely blocks compensatory synaptic vesicle endocytosis. *Proc Natl Acad Sci USA* **103:** 17955–17960

Pelkmans L, Helenius A (2003) Insider information: what viruses tell us about endocytosis. *Curr Opin Cell Biol* **15:** 414–422

Pelkmans L, Kartenbeck J, Helenius A (2001) Caveolar endocytosis of simian virus 40 reveals a new two-step vesicular-transport pathway to the ER. *Nat Cell Biol* **3:** 473–483

Polishchuk RS, Polishchuk EV, Marra P, Alberti S, Buccione R, Luini A, Mironov AA (2000) Correlative light-electron microscopy reveals the tubular-saccular ultrastructure of carriers operating between Golgi apparatus and plasma membrane. *J Cell Biol* **148:** 45–58

Praefcke GJ, McMahon HT (2004) The dynamin superfamily: universal membrane tubulation and fission molecules? *Nat Rev Mol Cell Biol* **5:** 133–147

Sabharanjak S, Sharma P, Parton RG, Mayor S (2002) GPI-anchored proteins are delivered to recycling endosomes via a distinct cdc42-regulated, clathrin-independent pinocytic pathway. *Dev Cell* **2:** 411–423

Schmid SL, McNiven MA, De Camilli P (1998) Dynamin and its partners: a progress report. *Curr Opin Cell Biol* **10:** 504–512

Schnatwinkel C, Christoforidis S, Lindsay MR, Uttenweiler-Joseph S, Wilm M, Parton RG, Zerial M (2004) The Rab5 effector Rabankyrin-5 regulates and coordinates different endocytic mechanisms. *PLoS Biol* **2:** E261

Steinman RM, Swanson J (1995) The endocytic activity of dendritic cells. *J Exp Med* **182:** 283–288

Swanson JA, Watts C (1995) Macropinocytosis. *Trends Cell Biol* **5:** 424–428

Upla P, Marjomaki V, Kankaanpaa P, Ivaska J, Hyypia T, Van Der Goot FG, Heino J (2004) Clustering induces a lateral redistribution of alpha 2 beta 1 integrin from membrane rafts to caveolae and subsequent protein kinase C-dependent internalization. *Mol Biol Cell* **15:** 625–636

Vecchi M, Polo S, Poupon V, van de Loo JW, Benmerah A, Di Fiore PP (2001) Nucleocytoplasmic shuttling of endocytic proteins. *J Cell Biol* **153:** 1511–1517

West MA, Bretscher MS, Watts C (1989) Distinct endocytotic pathways in epidermal growth factor-stimulated human carcinoma A431 cells. *J Cell Biol* **109:** 2731–2739

Yang JS, Lee SY, Spano S, Gad H, Zhang L, Nie Z, Bonazzi M, Corda D, Luini A, Hsu VW (2005) A role for BARS at the fission step of COPI vesicle formation from Golgi membrane. *EMBO J* **24:** 4133–4143